

Notes

Oxidative Decomposition of *Meso*-Azobis- α -phenylethane by Thianthrene Cation Radical

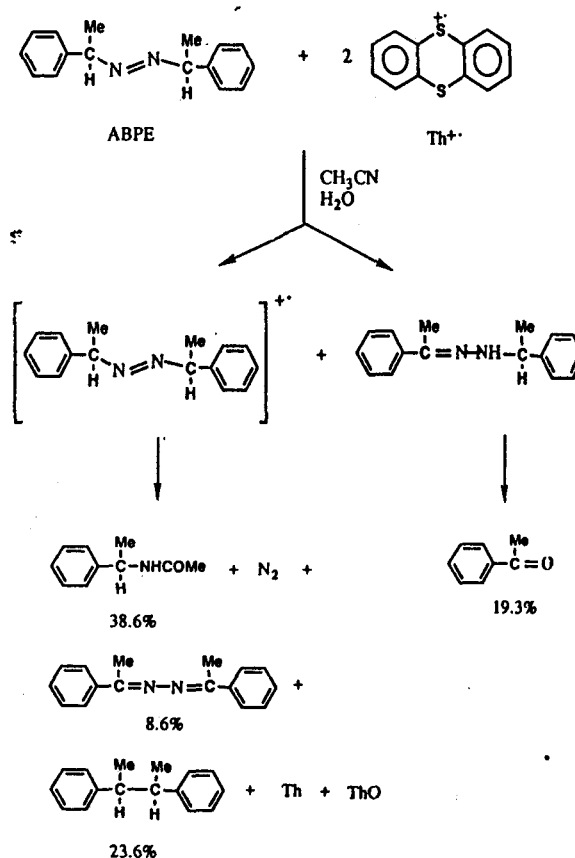
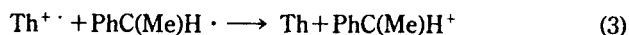
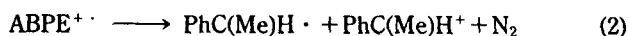
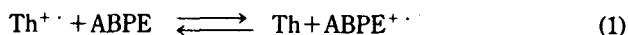
Wang Keun Lee* and Chun Taek Chung

Department of Chemistry Education,
Chonnam National University, Kwang-Ju 500-757

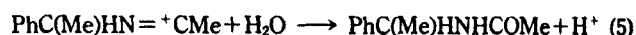
Received April 28, 1992

Cation radical-induced, oxidative chemistry of azoalkane has begun to emerge only in the last few years.¹⁻⁵ For example, azoalkane such as 1,1'-azoadamantane (AA), which has no α hydrogen, is oxidized by thianthrene cation radical perchlorate in acetonitrile solution, affording primarily nitrogen and cation-derived products.¹ However, 1,4-diphenylazomethane (DPAM) possessing two α hydrogens reacts with cation radicals and undergoes facile oxidative cycloaddition with the nitrile solvent to form 1,2,4-triazole.² The results from oxidation of AA and DPAM tell us quite clearly that the type of α -carbon in azoalkanes determines the products of oxidative cleavage. The present investigation arose from questions whether *meso*-azobis- α -phenylethane (ABPE) [1,1'-diphenylazoethane] possessing one α hydrogen is oxidized to its cation radical and decompose to liberate N₂, or tautomerized to its hydrazone and lead to oxidative cycloaddition to the nitrile solvent. The purpose of this study is to know the effects of structure on the oxidation of azoalkane and to validate the reaction mechanism which had been proposed for the oxidation of azoalkane by cation radical.

meso-ABPE undergoes thermolysis into α -phenylethyl radical in solution at reasonable rates at 100-160°C, leading to the 2,3-diphenylbutane (DPB) and rearranges to their hydrazone tautomer more readily than the simple aliphatic azo compounds.⁶ In contrast, this azoalkane reacted with thianthrene cation radical (Th^{•+}) at room temperature rapidly and evolved nitrogen and rearranged to a tautomer of *meso*-ABPE, acetophenone α -phenylethylhydrazone. While Th^{•+} was reduced quantitatively to thianthrene (Th), products from *meso*-ABPE, a traditional source of free radicals,⁷ were N- α -phenylethylacetamide (38.6%), 2,3-diphenylbutane (23.6%), acetophenone (19.3%) and acetophenone azine (8.6%). The overall view of the behavior of azoalkane in reaction with Th^{•+} can be explained by Scheme 1. Thus, the major initial trappable products of oxidative decomposition were the α -phenylethyl cations, which reacted with the solvent acetonitrile to give a Ritter-type intermediate PhC(Me)HN=⁺CMe. The Ritter-type intermediate reacted with water during workup to give N- α -phenylethylacetamide. One of the possible routes for the formation of the carbocationic product, N- α -phenylethylacetamide is shown in Eq. (1)-(5).



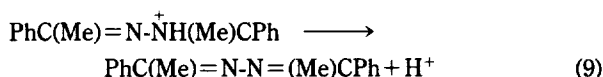
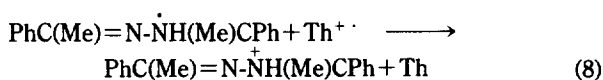
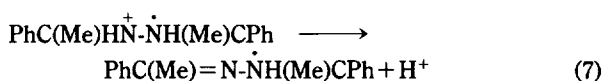
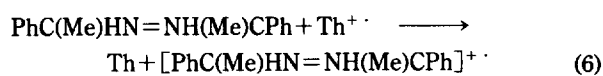
Scheme 1. Mechanism of product formation from *meso*-ABPE and thianthrene cation radical.



All these reactions may involve prior complexation, as was proposed for the cation radical oxidation of anisole.⁸

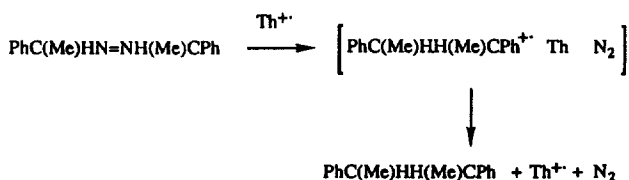
In contrast to the oxidation of AA, and of DPAM with cation radical, acetophenone and small amounts of azine, PhC(Me)=N-N=(Me)CPh were obtained. The formation of acetophenone can be attributed to the hydrolysis of either the corresponding hydrazone or acetophenone azine. However, when an attempt was made to hydrolyze the authentic azine by 70% perchloric acid in acetonitrile solution, the azine was recovered quantitatively. Hence, the formation of acetophenone from the hydrolysis of the azine can be ruled out. Azoalkanes possessing α -protons can tautomerize easily to the more stable isomeric hydrazones.⁹ We are not sure whether the tautomerization occurred in solution prior to the oxidation of *meso*-ABPE or after oxidation, but the cation radical of *meso*-ABPE tautomerized to the cation radical of acetophenone α -phenylethylhydrazone. In this study, 1,2,4-triazole can't be formed from the oxidative cycloaddition of acetophenone α -phenylethylhydrazone cation radical to the solvent MeCN, because ABPE has only one α hydrogen. Acetophenone azine was a product of oxidation of the azo com-

pound. A possible mechanism for the formation of the azine is shown in Eq. (6)-(9).



The formation of the thianthrene 5-oxide (ThO) can be rationalized by hydrolysis of either some of $\text{Th}^{+\cdot}$ by incompletely dried solvent during the course of reaction, or unused $\text{Th}^{+\cdot}$ during workup.¹⁰

No evidence for ethylbenzene was found from the α -phenylethyl radical disproportionation reaction or from hydrogen abstraction from MeCN. When the reaction of $\text{Th}^{+\cdot}$ with *meso*-ABPE was carried out in the presence of BrCCl_3 in MeCN, as we did earlier with AA, the formation of DBP was not stopped. Therefore, we can conclude that DPB is probably not formed in the oxidative reactions by dimerization of α -phenylethyl radical. Generally, radical is destined to abstract hydrogen atom from MeCN rather than to dimerize in the absence of a competing reaction.¹¹ The mechanism for the formation of DPB is rationalized in Scheme 2, which is very similar to that of formation of AdAd by $\text{Th}^{+\cdot}$.¹¹ DPB may have arisen from the DPB cation radical $[\text{PhC(Me)HH}(\text{Me})\text{CPh}]^{+\cdot}$, formed by a cage recombination between α -phenylethyl cation and α -phenylethyl radical, rather than the coupling between two α -phenylethyl radicals. Conversion of DPB cation radical into DPB would have to occur by electron-transfer reaction from $\text{Th}^{+\cdot}$ within solvent cage. In that case, $\text{Th}^{+\cdot}$ would have served as a catalyst for the formation of DPB from *meso*-ABPE. It is interesting to compare the yield of AdAd and DPB from oxidative decomposition of corresponding azoalkane $\text{Th}^{+\cdot}$. Whereas 2.5% of AdAd was obtained from oxidation of AA, 23.6% of DPB was formed in the oxidative of *meso*-ABPE by $\text{Th}^{+\cdot}$. In the oxidation of *meso*-ABPE with $\text{Th}^{+\cdot}$, α -phenylethyl radical would not survive so long enough to be reduced to cation as tertiary adamantyl radical. Therefore, relatively lots of α -phenylethyl radical would recombine with α -phenylethyl cation to form a DPB without further oxidation in the solvent cage. *Meso*-ABPE gave 21.8% of *meso* and 1.8% of non-*meso*-DPB, indicating that some changes in orientations (by out-of-plane rotation) of the cations and radicals are occurring in these original cages prior to combination between α -phenylethylcation and



Scheme 2. Possible reaction pathways for the formation of 2,3-diphenylbutane.

α -phenylethyl radical.

In conclusion, the reaction of $\text{Th}^{+\cdot}$ with *meso*-ABPE, possessing one α hydrogen, in acetonitrile follows not only the carbocationic route but also undergoes tautomerization to its hydrazone, and no oxidative cycloaddition was observed.

Acknowledgement. We thank the Chonnam National University for financial support (1991) and acknowledge Dr. Sung Sik Kim of Conbuk National University for GC-MS.

References

- D. H. Bae, P. S. Engel, A. K. M. M. Hoque, D. E. Keys, W. K. Lee, R. W. Shaw, and H. J. Shine, *J. Am. Chem. Soc.*, **107**, 2561 (1985).
 - A. K. M. M. Hoque, A. C. Kovelesky, W. K. Lee, and H. J. Shine, *Tetrahedron Lett.*, 5655 (1985).
 - H. J. Shine, D. H. Bae, A. K. M. M. Hoque, A. Kajstura, W. K. Lee, R. W. Shaw, M. Soroka, P. S. Engel, and D. E. Keys, *Phosphorus sulfur*, **23**, 111 (1985).
 - J. M. Lee, K. Kim, and J. H. Shin, *Bull. Korean Chem. Soc.*, **6**, 358 (1985).
 - P. S. Engel, A. K. M. M. Hoque, J. N. Scholz, H. I. Shine, and K. H. Witmire, *J. Am. Chem. Soc.*, **110**, 7880 (1988).
 - S. G. Cohen, S. J. Groszos, and D. B. Sparrow, *J. Am. Chem. Soc.*, **72**, 3947 (1960).
 - P. S. Engel, *Chem. Rev.*, **99**, 80 (1980).
 - O. Hammerich and V. D. Parker, *Adv. Phys. Org. Chem.*, **20**, 55 (1984).
 - P. A. S. Smith, *Derivatives of Hydrazine and other Hydronitrogens having N-N Bonds: Benjamin/Cummings: Reading, Mass.*, pp. 47-70, 176-177, 1983.
 - Y. Murata and H. J. Shine, *J. Org. Chem.*, **34**, 3368 (1969).
- Caution:** $\text{Th}^{+\cdot}\text{ClO}_4^-$ is explosive. It should be prepared in small quantities only and used soon after preparation. Sintered glass should not be used for filtration.
- P. S. Engel, W. K. Lee, G. E. Marschke, and H. J. Shine, *J. Org. Chem.*, **52**, 2813 (1987).

The Crystal Structure and Magnetic Properties of Triethylenediaminenickel(II)-Bis(maleonitriledithiolato)nickelate(II); $[\text{Ni}(\text{C}_2\text{H}_5\text{N}_2)_3] \cdot [\text{Ni}(\text{C}_4\text{N}_2\text{S}_2)_2]$

Chulmin Keum, CHonhan Kim, Chulsung Kim, Hyontae Kwak, Moonhee Kwon, and Hae Namgung[†]

Department of Chemical Education, Kookmin University, Seoul 136-702

[†]Department of Physic Education, Kookmin University, 136-702

Received June 3, 1992

Bidentate dithiolate ligands form very well square planar complexes with Ni-triad ions of different oxidation states,

Table 1. Experiment Data for the X-ray Diffraction Study

$a=8.719(3)$ Å	Crystal	= Red, Needle
$b=9.556(3)$ Å	Formula	= $\text{Ni}_2\text{C}_{14}\text{H}_{24}\text{N}_{10}\text{S}_4$
$c=16.279(4)$ Å	Space Group	= $\overline{P}1$ (No=2)
$\alpha=85.74(2)^\circ$	Z	= 2
$\beta=99.38(2)^\circ$	Mol. Wt.	= 578.09
$\gamma=117.14(2)^\circ$	D_c	= 1.612 g cm^{-3}
$V=1190.8 \text{ cm}^3$	μ	= 19.5 cm^{-1}
	$F_{(000)}$	= 596
Radiation		= Mo-K α , 0.7107 Å
Monochromator		= Incident beam, Graphite
Mode		= $\theta/2\theta$
2θ range ($^\circ$)		= $2-50^\circ$
HKL ranges		= H -10 to 10
		K 0 to 10
		L -19 to 19
Correction		= Lorentz, Polarisation, Linear decay (averaging 1.00163 on I)
Reflection		= 4344 total
		= 4187 unique
		= 3418 used with $I > 3.0 \sigma(I)$
Parameter refined		= 376
R, wR, R (all)		= 0.046, 0.065, 0.071
Maximum shift e.s.d		= 0.03
Scale factor (final)		= 0.297
Goodness of fit		= 1.76
$\Delta\rho$		= $0.611 \text{ e}\text{\AA}^{-3}$

whose solid state properties exhibit widespread electrical behavior from insulating through semiconducting to metallic.¹ The high metallic conductive complex $\text{Li}_{0.75}[\text{Pt}(\text{mnt})_2] \cdot 2\text{H}_2\text{O}$ ($\text{mnt}=1,2$ -Dicyanoethylene-1,2-dithiolate) has an one-dimensional columnar structure similar to those of the partially oxidized tetracyanoplatinate and bis (oxalato)-platinate complexes.² The semiconducting complex of $(\text{C}_2\text{H}_5)_4\text{N} \cdot [\text{Ni}(\text{mnt})_2]$ also shows the one-dimensional stacks of coplanar overlapped diadic anion unit.³ The electrically insulating complex of $[(\text{C}_4\text{H}_9)_4\text{N}]_2 \cdot [\text{Ni}(\text{mnt})_2]$ is isomorphous with Co^{2+} and Cu^{2+} complexes with large metal to metal distances.⁴ In our investigation of the influence of the Ni-triadic complex cations, instead of oxonium ions as counter ion, on the stacking structure of $\text{M}(\text{mnt})_2^{2-}$ anions with different oxidation states ($x=1$ - or 2 -) within a crystal, most of complexes prepared were obtained as powder and only single crystals of the title complex were suitable for X-ray structure analysis. We report here its crystal structure and magnetic properties.

$[\text{Ni}(\text{en})_3] \cdot [\text{Ni}(\text{mnt})_2]$. The preparations of the starting compounds, $\text{Ni}(\text{en})_3 \cdot (\text{ClO}_4)_2$ and $(\text{Et}_4\text{N})_2 \cdot \text{Ni}(\text{mnt})_2$, were carried out according to the literature procedures.⁵ The red-orange compounds of $\text{Ni}(\text{en})_3 \cdot \text{Ni}(\text{mnt})_2$ was obtained by mixing of the two equimolar solutions of tris(ethylenediamine) nickel(II) perchlorate and bis(tetraethylammonium) bis (1,2-dicyanoethylene dithiolato) nickelate(II) in boiling methanol. The red needle single crystals were obtained by recrystallization from the mixed solvent of $\text{CH}_3\text{CN}/\text{CH}_3\text{OH}/\text{H}_2\text{O}$.

X-ray Crystal Structure Determination. A crystal was mounted on an Enraf-Norius CAD4-diffractometer using

Table 2. Atomic Coordinates and equivalent Isotropic Thermal Parameters of Nonhydrogen Atoms

Atom	X	Y	Z	B (\AA^2)
Ni-1	0.000	0.000	0.000	4.10(3)
S1	-0.0841(3)	0.1288(2)	-0.0975(1)	4.82(5)
S2	0.1940(3)	0.2146(2)	0.0627(1)	5.08(5)
C1	0.0472(9)	0.3233(8)	-0.0674(5)	4.3(2)
C2	0.1667(9)	0.3583(8)	0.0015(5)	4.4(2)
C3	0.019(1)	0.4414(9)	-0.1179(5)	5.0(2)
C4	0.278(1)	0.5172(9)	0.0269(5)	4.9(2)
N1	-0.006(1)	0.5345(8)	-0.1582(5)	6.9(2)
N2	0.369(1)	0.6436(8)	0.0492(5)	6.4(2)
Ni-2	0.500	0.000	0.500	4.11(3)
S3	0.7128(3)	0.1288(2)	0.5973(1)	4.79(5)
S4	0.5207(3)	0.2146(2)	0.4372(1)	5.06(5)
C5	0.7767(9)	0.3230(8)	0.5676(5)	4.2(2)
C6	0.6917(9)	0.3585(8)	0.4982(5)	4.3(2)
C7	0.922(1)	0.4414(8)	0.6177(5)	4.9(2)
C8	0.740(1)	0.5177(8)	0.4731(5)	4.8(2)
N3	1.040(1)	0.5352(9)	0.6582(5)	6.8(2)
N4	0.775(1)	0.6442(7)	0.4510(5)	6.4(2)
Ni-3	0.7229(1)	-0.05429(9)	0.25003(6)	3.44(2)
N5	0.6945(8)	-0.0377(7)	0.1199(4)	5.1(2)
N6	0.6367(9)	0.1217(7)	0.2368(5)	6.2(2)
N7	0.7673(8)	-0.0378(7)	0.3793(4)	5.1(2)
N8	0.9846(9)	0.1212(8)	0.2631(5)	6.2(2)
N9	0.7870(8)	-0.2431(7)	0.2542(4)	5.2(2)
N10	0.4694(8)	-0.2436(8)	0.2459(4)	5.3(2)
C9	0.676(2)	0.099(1)	0.0950(7)	8.6(3)
C10	0.585(1)	0.137(1)	0.1473(7)	7.8(3)
C11	0.922(2)	0.099(1)	0.4047(7)	8.7(4)
C12	1.053(1)	0.138(1)	0.3512(7)	7.9(3)
C13	0.627(1)	-0.3892(9)	0.2311(7)	6.9(3)
C14	0.484(1)	-0.389(1)	0.2695(7)	6.9(3)

Anisotropically refined atoms are given in the form of the isotropic equivalent displacement parameter defined as: $(4/3) \times [a^2 \times B(1, 1) + b^2 \times B(2, 2) + c^2 \times B(3, 3) + ab(\cos \gamma) \times B(1, 2) + ac(\cos \beta) \times B(1, 3) + bc(\cos \alpha) \times B(2, 3)]$

graphite monochromated Mo-K α radiation. The unit cell dimensions and an orientation matrix were obtained from a least-squares refinement of the setting angles of 25 reflections with $5.06 < 2\theta < 35.50^\circ$. The cell parameters and other crystallographic data are given in Table 1. The intensities of three standard reflections (002, 040, 371) were measured after every one hour during the data collection. Intensities of these standard reflections remained constant within 0.007 % per hour throughout the data collection. The data were corrected for Lorentz and polarisation effect. The 3418 reflections with $I > 3.0\sigma(I)$ were used in the subsequent analysis. The structure was solved by Patterson methods and fourier maps using SHELXS⁶ and SDP⁷ package programmes on PC and PDP 11/23+ computers.

All the nonhydrogen atoms were found from a three dimensional fourier maps and refined anisotropically by full-matrix least squares calculations on F_o 's. The function $\sum w(F_o - F_c)^2$

Table 3. Bond Distances (Å) and Bond Angles (°) with e.s.d.'s in Parentheses

A: Bond distances (Å)					
Ni-1 -S1	2.174(2)	S3 -C5	1.733(6)	Ni-3 -N9	2.11(1)
Ni-1 -S2	2.166(2)	S4 -C6	1.717(6)	Ni-3 -N10	2.118(7)
S1 -C1	1.737(6)	C5 -C6	1.356(8)	N5 -C9	1.405(8)
S2 -C2	1.718(6)	C5 -C7	1.431(9)	C9 -C10	1.428(8)
C1 -C2	1.347(8)	C6 -C8	1.428(8)	C10 -N6	1.471(9)
C1 -C3	1.43(1)	C7 -N3	1.151(8)	N7 -C11	1.408(8)
C2 -C4	1.426(9)	C8 -N4	1.148(7)	C11 -C12	1.44(1)
C3 -N1	1.144(8)	Ni-3 -N5	2.095(5)	C12 -N8	1.46(1)
C4 -N2	1.149(7)	Ni-3 -N6	2.118(6)	N9 -C13	1.47(1)
Ni-2 -S3	2.172(2)	Ni-3 -N7	2.082(5)	C13 -C14	1.48(1)
Ni-2 -S4	2.167(2)	Ni-3 -N8	2.113(9)	C14 -N10	1.47(2)
B: Bond Angles (°)					
S1 -Ni-1 -S2	92.29(7)	S3 -C5 -C7	117.5(5)	N7 -Ni-3 -N9	91.6(3)
S1 -Ni-1 -S2'	87.71(7)	C6 -C5 -C7	122.3(5)	N7 -Ni-3 -N10	94.2(3)
Ni-1 -S1 -C1	102.7(2)	S4 -C6 -C5	121.7(5)	N8 -Ni-3 -N9	94.5(4)
Ni-1 -S2 -C2	102.8(3)	S4 -C6 -C8	117.1(5)	N8 -Ni-3 -N10	174.2(3)
S1 -C1 -C2	120.3(5)	C5 -C6 -C8	121.4(6)	N9 -Ni-3 -N10	81.0(4)
S1 -C1 -C3	117.1(5)	C5 -C7 -N3	179.2(7)	Ni-3 -N5 -C9	109.5(5)
C2 -C1 -C3	122.6(5)	C6 -C8 -N4	178.2(8)	N5 -C9 -C10	113.6(5)
S2 -C2 -C1	121.9(5)	N5 -Ni-3 -N6	82.0(2)	C9 -C10 -N6	113.9(6)
S2 -C2 -C4	116.8(5)	N5 -Ni-3 -N7	172.3(3)	Ni-3 -N6 -C10	107.3(4)
C1 -C2 -C4	121.4(6)	N5 -Ni-3 -N8	92.6(3)	Ni-3 -N7 -C11	109.7(4)
C1 -C3 -N1	179.1(8)	N5 -Ni-3 -N9	94.3(3)	N7 -C11 -C12	113.3(6)
C2 -C4 -N2	178.0(8)	N5 -Ni-3 -N10	91.6(3)	C11 -C12 -N8	113.9(8)
S3 -Ni-2 -S4	92.31(7)	N6 -Ni-3 -N7	92.5(2)	Ni-3 -N8 -C12	107.9(6)
S3 -Ni-2 -S4'	87.70(7)	N6 -Ni-3 -N8	90.1(3)	Ni-3 -N9 -C13	109.1(7)
Ni-2 -S3 -C5	102.9(2)	N6 -Ni-3 -N9	174.2(3)	N9 -C13 -C14	108.9(7)
Ni-2 -S4 -C6	102.9(3)	N6 -Ni-3 -N10	94.5(3)	C13 -C14 -N10	109.1(7)
S3 -C5 -C6	120.2(5)	N7 -Ni-3 -N8	82.1(3)	Ni-3 -N10 -C14	108.8(5)
C: β angles (°) (torsion angle) and Hydrogen bonds (Å)					
N5 -C9 -C10 -N2	43.6(1.2)				
N7 -C11 -C12 -N4	42.4(1.3)				
N9 -C13 -C14 -N6	53.9(1.0)				
		N—H	H—N	<NHN	N—N
N5 -H1 — N2*		1.006(5)	2.195(6)	173.0(5) ^p	3.196(8)
N7 -H9 — N3*		1.008(7)	2.195(6)	173.7(4) ^p	3.20(8)
N9 -H1 — N2*		1.009(5)	2.451(6)	142.1(4) ^p	3.3(1)
N10 -H23 — N2*		1.009(6)	2.449(6)	142.3(6) ^p	3.31(1)

*: Symmetry code 10-10.

F_o^2 was minimized with unit weights. The positional parameters of the hydrogen atoms were calculated with idealized bond length (1.0 Å). After one cyclic refinement of all atomic parameters with anisotropic temperature factors for all the nonhydrogen atoms and fixed isotropic ones for hydrogen atoms, the final results of structure solution are given in Table 1. The final atomic coordinates and the equivalent isotropic thermal parameters of the nonhydrogen atoms are listed in Table 2. The anisotropic thermal parameters of nonhydrogen atoms, the atomic coordinates and isotropic thermal parameters of hydrogen atoms, the least square planes and dihedral angles, the final values of observed and calculated

structure factors are listed in Tables from S1 to S4.⁸

Magnetic Susceptibility Measurement. Static magnetic susceptibility data were collected in the temperature range 10-269K on a powdered sample by using a MPMS-SQUID-magnetometer (Quantum Design Inc., USA). The sample weights and applied fields used were 9 mg and 5000 Gauss. The effective magnetic moments of 2.85 B.M. at 269 K are calculated by using the formula, $\mu_{eff} = 2.83\sqrt{\chi_m \cdot T}$ where χ_m is molar magnetic susceptibility per a molecule corrected for diamagnetism for all the constituent atoms of 1,2-ethylenediamine by the use of Pascal's constant.⁹ The electric conductance was not measured as the compound was expected

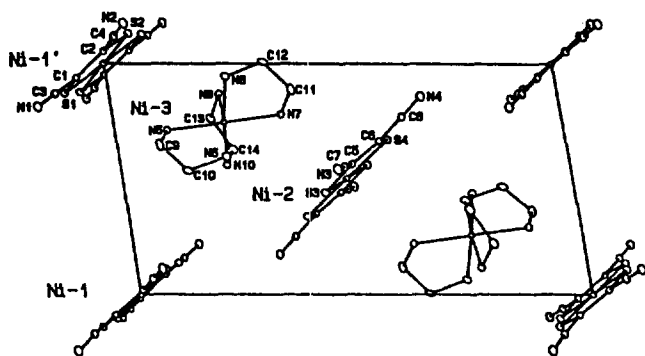


Figure 1. Projection of packing arrangement with atomic numbering. The unit cell is oriented with +c axis horizontal, the +a axis vertical and the +b axis pointing toward the reader.

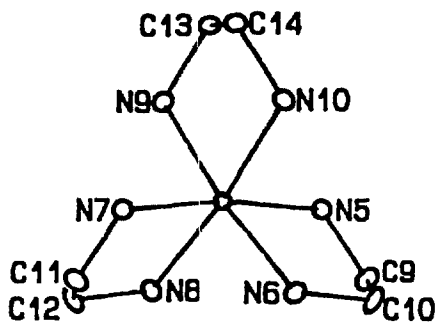


Figure 2. View of the $\text{Ni}(\text{en})_3^{2+}$ cation. The configuration shown is $\Lambda(\delta\delta\delta)$, but in this centrosymmetric structure there are an equal number of $\Delta(\lambda\lambda\lambda)$ configurations. The last ring is the central ring (Ni-N9-C13-C14-N10-Ni). The hydrogen atoms are not shown.

to be electric insulator.

Results and Discussion

The unit cell consist of two crystallographically independent $\text{Ni}(\text{mnt})_2^{2-}$ ions and a $\text{Ni}(\text{en})_3^{2+}$ ion. The bond lengths and angles of the complex are listed in Table 3 and their corresponding e.s.d.'s are shown in parentheses. An ORTEP¹⁰ crystal packing diagram with atomic numbering scheme is shown in Figure 1. The central Ni-atoms of two $\text{Ni}(\text{mnt})_2^{2-}$ are placed on the projection plane, but two Ni-atoms of $\text{Ni}(\text{en})_3^{2+}$ which are related by an inversion center, are deviated very slightly up and down from the plane. Although two averaged Ni-S bond lengths (2.173 and 2.167 Å) are larger than those of $\text{Ni}(\text{mnt})_2^{1-}$ anions,^{3,11} they are somewhat larger or smaller than those of $\text{Ni}(\text{mnt})_2^{2-}$ anions in other structures.^{3,12} The ring of the Ni-2 complex anion has larger deviations than that of the Ni-1 complex from the least square planes of $\text{Ni}(\text{mnt})_2^{2-}$ ions which are assumed essentially planar. The dihedral angle between the two least square planes is 11.7°. The configuration of $\text{Ni}(\text{en})_3^{2+}$ complex cation viewed down the pseudo threefold axis of the nickel ion is shown in Figure 2. The figure shows that the ethylenediamine chelate rings have identical conformations and three carbon-carbon bonds of ethylenediamine groups are almost parallel to the threefold axis. Therefore, the configuration of this cation may be described as $\Lambda(\delta\delta\delta)$; in this centrosym-

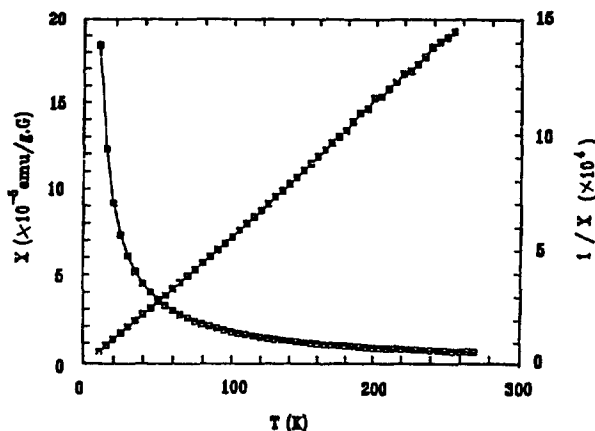


Figure 3. Temperature dependence of the gram magnetic susceptibility χ_g and the inverse susceptibility.

metric space group there are also equal number of the cation with enantiomeric $\Delta(\lambda\lambda\lambda)$ form. All of the known configurations of $[\text{Ni}(\text{en})_3]^{2+}$ cations,¹³ which form salts with sulfate and nitrate ions, but not involving any water molecules, have been reported to be $\Lambda(\delta\delta\delta)$ as in this complex.

Corey and Bailar¹⁴ calculated that the most stable configuration for $[\text{M}(\text{en})_3]^{n+}$ ion is $\Lambda(\delta\delta\delta)$. However, the configurations of $[\text{Cr}(\text{en})_3]^{3+}$ anions¹⁵ were reported as $\Lambda(\delta\lambda\lambda)$, $\Lambda(\delta\delta\lambda)$ and $\Lambda(\lambda\lambda\lambda)$, but these complexes have one and half more hydrate water molecules. Raymond *et al.*^{15a} proposed that the higher energy conformers are stabilized by hydrogen bonds. They found the $\Lambda(\delta\delta\lambda)$ conformer involved in three strong hydrogen bonds, the $\Lambda(\delta\lambda\lambda)$ conformer in seven and the $\Lambda(\lambda\lambda\lambda)$ conformer in ten hydrogen bonds.

In order to confirm the above proposed configuration of $\text{Ni}(\text{en})_3^{2+}$ cation of the title complex, the following factors were compared and calculated with each other in details. The bond distances and angles of the third conformation (N9-C13 1.47, C13-C14 1.48 Å, N9-C13-C14 108.9, C13-C14-N10 109.1°) of $\text{Ni}(\text{en})_3^{2+}$ configuration were essentially deviated larger than the corresponding averaged values (1.407, 1.434 Å, 113.5, 113.9°) of two other conformations. So then, we calculate the dihedral angle α between the plane which contains the ring carbon atoms and the metal atom and the plane which contains the ring nitrogen atoms and the metal atom and also the angles β between the two nitrogen atoms as one looks down the carbon-carbon bond.

The angles α and β of three conformations were responded to 21 and 43.6 for A, 20 and 42.4 for B, 27.3 and 53.9° for C ring respectively. On the other hand, two or four weak hydrogen bonds between nitrogen atoms of cations and nitrogen atoms of neighboring anions are possible, when NN bond lengths of hydrogen bonds are assumed to be less than 3.4 Å. The distances between two nitrogen atoms of first two conformations of complex cation and two nitrogen atoms of two complex anions are closer than those of the last conformation. Even through it may be proposed as $\Lambda(\delta\delta\lambda)$ instead of $\Lambda(\delta\delta\delta)$, based on the above discussions for the configuration of $\text{Ni}(\text{en})_3^{2+}$ ion, it should be described as $\Lambda(\delta\delta\delta)$ on account of the positive values of the all angles of α and β .

The gram magnetic susceptibility of a powdered samples is plotted as a function of temperature in Figure 3. The in-

verse magnetic susceptibility is fitted excellently to a straight line in the temperature range 10-269 K. The susceptibility exhibits typical Curie law dependence, with the Curie constant of $1.014 \text{ emu K mol}^{-1}$.

Acknowledgement. This work was supported by a grant from the Basic Research Institute Program (1992), Ministry of Education, Republic of Korea.

References

- (a) J. F. Wheiber, L. R. Melby, and R. E. Benson, *J. Amer. Chem. Soc.*, **86**, 4329 (1964); (b) A. E. Underhill and M. M. Ahmad, *JCS Chem. Comm.*, 67 (1981); (c) M. M. Ahmad and A. E. Underhill, *JCS Chem. Comm.*, 1065 (1982); (d) L. C. Isett, D. M. Rosso, and G. L. Bottger, *Phys. Rev.*, **22B**, 4739 (1980).
- (a) K. Krogmann, *Angew. Chem. Int. Ed. Engl.*, **8**, 35 (1969); (b) M. J. Minot and J. H. Perstein, *Phys. Rev. Lett.*, **26**, 371 (1971); (c) K. Krogmann, *Z. Anorg. Allg. Chem.*, **358**, 97 (1968); (d) A. H. Reis, Jr., S. W. Peterson, and S. C. Lin, *J. Amer. Chem. Soc.*, **98**, 7839 (1976).
- A. Kobayashi and Y. Sasaki, *Bull. Chem. Soc. Jpn.*, **50**, 2650 (1977).
- (a) J. D. Forrester, A. Zalkin, and D. H. Templeton, *Inorg. Chem.*, **3**, 1500 (1964); (b) J. D. Forrester, A. Zalkin, and D. H. Templeton, *Inorg. Chem.*, **3**, 1507 (1964); (c) K. W. Plumlee, B. M. Hoffman, J. A. Ibers, and Z. G. Soos, *J. Chem. Phys.*, **63**, 1926 (1975).
- (a) M. E. Farago, J. M. James, and V. C. G. Trew, *J. Chem. Soc.*, **A**, 820 (1969); (b) E. Billig, R. Williams, Z. Bernal, J. H. Waters, and H. B. Gray, *Inorg. Chem.*, **3**, 663 (1964).
- G. M. Sheldrick, (1986), **SHELXS**, Program for Crystal Structure Determination, University of Cambridge, England.
- B. A. Frenz, Enraf-Nonius **SDP-PLUS** Structure Determination Package, Version 3.0, Enraf-Nonius, Delft, The Netherlands (1985).
- Supplementary materials. These are available from the corresponding author upon request.
- (a) A. Weiss and H. Witte, "Magnetochemie", Verlag Chemie, Weinheim/Germany, 136 (1972); (b) R. L. Carlin, "Magnetochemistry", Springer-Verlag, Berlin/Germany, 3 (1986).
- C. K. Johnson, **ORTEP**, Report **ORNL-3794**, Oak Ridge National Laboratory, Tennessee, USA (1965).
- C. J. Fritchie, Jr., *Acta Cryst.*, **20**, 107 (1966).
- (a) M. T. Hove, B. M. Hoffmann, and J. A. Ibers, *J. Chem. Phys.*, **56**, 3490 (1972); (b) R. Eisenberg, J. A. Ibers, R. J. H. Clark, and H. B. Gray, *J. Amer. Chem. Soc.*, **86**, 113 (1964).
- (a) L. N. Swink and M. Atoji, *Acta Cryst.*, **13**, 639 (1960); (b) M. U. Haque, C. N. Caughlan, and K. Emerson, *Inorg. Chem.*, **9**, 2421 (1970).
- E. J. Corey and J. C. Bailar, Jr., *J. Amer. Chem. Soc.*, **81**, 2620 (1959).
- (a) K. N. Raymond, P. W. R. Corfield, and J. A. Iberg, *Inorg. Chem.*, **7**, 842 (1968); (b) K. N. Raymond, P. W. R. Corfield, and J. A. Iberg, *Inorg. Chem.*, **7**, 1362 (1968).

Valence States of SH^{2+} by *Ab Initio* Effective Valence Shell Hamiltonian

Jong Keun Park and Hosung Sun*

Department of Chemistry, Pusan National University,
Pusan 609-735

Received June 19, 1992

Recently the electronic states of doubly positive diatomic cations have been investigated extensively^{1,2}. In those studies a few quasibound states of doubly positive diatomic cations have been found. There is a repulsive force between two singly positive monatomic cations. The repulsive force is overcome sometimes by redistribution of electron densities when a doubly positive diatomic cation is formed. Therefore metastable bound states can exist in some cases. In other words the avoided curve crossing between a state arising from an ion-ion asymptote (dissociation limit) and a state with the same symmetry arising from an ion-neutral asymptote is a main reason for the existence of quasibound states in doubly positive diatomic cations.

We have studied the nature of the effective valence shell Hamiltonian (H^p) which is based on the quasidegenerate many-body perturbation theory³. One of remarkable features of H^p is that the effective H^p operator can reproduce all the valence states of a neutral molecule and its ions simultaneously regardless of its charge states. Once the matrix elements of H^p are evaluated for a neutral molecule, the same matrix elements can be used to determine the valence states of its singly positive, doubly positive, ... cations.

The existence of the bound states in NO^{2+} , O_2^{2+} , etc. may be easily predicted. But for the first row diatomic monohydrides, say, CH^{2+} , or NH^{2+} cation, the existence of unusually stable states may not be easily understood. If two electrons are removed from the $1\pi^2$ orbital of neutral NH, NH^{2+} may exist because the 1π orbital of neutral NH has basically non-bonding character. For CH^{2+} , the prediction of its existence is not so simple because at least one electron should be removed from a bonding 3σ orbital of neutral CH to form CH^{2+} cation. We have previously studied the CH^{2+} cation and found no bound states.⁴ Therefore so far the H^p has been mainly applied to neutral molecules and singly positive cations. But recently doubly positive cations of various second row diatomic monohydrides have been studied by configuration interaction (CI) method^{5,6}. We are encouraged by these studies so that now we apply the H^p method to these systems.

In the present work, we have performed H^p calculations on the SH^{2+} cation. The SH^{2+} cation has been studied previously^{2,6}. But one should note that a single H^p calculation simultaneously produces all the valence state energies with same accuracy. So that our present H^p calculations reveal a composite picture of the SH^{2+} potential energy curves of all the valence states.

The second order effective valence shell Hamiltonian calculations for SH^{2+} are performed with a contracted Gaussian basis set of $[7s5p3d]$ for sulfur and $[2s1p]$ for hydrogen⁷. Molecular orbitals are obtained from the SCF (self-consistent-